

Automatic calculation of myocardial external efficiency using a single ^{11}C -acetate PET scan

Hendrik J. Harms, PhD,^a Nils Henrik S. Hansson, MD, PhD,^b Tanja Kero, MD,^c Tomasz Baron, MD, PhD,^d Lars P. Tolbod, PhD,^a Won Y. Kim, MD, PhD,^b Jørgen Frøkiær, MD, PhD,^a Frank A. Flachskampf, MD, PhD,^d Henrik Wiggers, MD, PhD,^b and Jens Sørensen, MD, PhD^{a,c}

^a Department of Nuclear Medicine, & PET Center, Aarhus University Hospital, Aarhus N, Denmark

^b Department of Cardiology, Aarhus University Hospital, Aarhus, Denmark

^c Department of Nuclear Medicine & PET, Uppsala University Hospital, Uppsala, Sweden

^d Department of Medical Sciences, Uppsala Clinical Research Center, Uppsala University, Uppsala, Sweden

Received Jan 16, 2018; accepted Apr 25, 2018

doi:10.1007/s12350-018-1338-0

Background. Myocardial external efficiency (MEE) is defined as the ratio of kinetic energy associated with cardiac work [forward cardiac output (FCO)*mean systemic pressure] and the chemical energy from oxygen consumed (MVO_2) by the left ventricular mass (LVM). We developed a fully automated method for estimating MEE based on a single ^{11}C -acetate PET scan without ECG-gating.

Methods and Results. Ten healthy controls, 34 patients with aortic valve stenosis (AVS), and 20 patients with mitral valve regurgitation (MVR) were recruited in a dual-center study. MVO_2 was calculated using washout of ^{11}C -acetate activity. FCO and LVM were calculated automatically using dynamic PET and parametric image formation. FCO and LVM were also obtained using cardiac magnetic resonance (CMR) in all subjects. The correlation between $\text{MEE}_{\text{PET-CMR}}$ and MEE_{PET} was high ($r = 0.85$, $P < 0.001$) without significant bias. MEE_{PET} was $23.6 \pm 4.2\%$ for controls and was lowered in AVS ($17.2 \pm 4.3\%$, $P < 0.001$) and in MVR ($18.0 \pm 5.2\%$, $P = 0.004$). MEE_{PET} was strongly associated with both NYHA class ($P < 0.001$) and the magnitude of valvular dysfunction (mean aortic gradient: $P < 0.001$, regurgitant fraction: $P = 0.009$).

Conclusion. A single ^{11}C -acetate PET yields accurate and automated MEE results on different scanners. MEE might provide an unbiased measurement of the phenotypic response to valvular disease. (J Nucl Cardiol 2018;25:1937–44.)

Key Words: Myocardial efficiency • myocardial energetics • positron emission tomography • ^{11}C -acetate

Electronic supplementary material The online version of this article (<https://doi.org/10.1007/s12350-018-1338-0>) contains supplementary material, which is available to authorized users.

Reprint requests: Jens Sørensen, MD, PhD, Department of Nuclear Medicine & PET, Uppsala University Hospital, Uppsala, Sweden; jens.sorensen@pet.uu.se

1071-3581/\$34.00

Copyright © 2018 The Author(s)

Abbreviations

MEE	Myocardial external efficiency
TE	Total energy use
EW	External work
LVM	Left ventricular mass
FCO	Forward cardiac output
MVO ₂	Myocardial oxygen consumption
CMR	Cardiac magnetic resonance imaging
PET	Positron emission tomography
AVS	Aortic valve stenosis
MVR	Mitral valve regurgitation

See related editorial, pp. 1945–1947

INTRODUCTION

A common feature in most cardiomyopathies is a reduction in myocardial external efficiency (MEE)¹ i.e., an imbalance between cardiac work and total energy consumption by the left ventricle (LV). MEE reflects both mechanical performance and metabolic integrity. A reduction in MEE may result from ischemia, increased wall stress or filling pressures and leads to a further deterioration of LV function. Preserving or restoring MEE is associated with better prognosis and a reduction of symptoms in patients with left ventricular systolic dysfunction,² dilated cardiomyopathy,^{3,4} aortic valve stenosis,⁵ and hypertrophic cardiomyopathy⁶ and was thus suggested as a therapeutic target. In addition, MEE may serve as an early marker of cardiac performance and can potentially be used as a more sensitive marker of interventions.^{7,8}

The gold standard for measuring MEE makes use of pressure-volume loops and the Fick-principle to estimate cardiac work and myocardial oxygen consumption (MVO₂), respectively. However, the requirement for dual-sided catheterization has ruled out this method in a clinical setting. Accurate non-invasive alternatives are available,⁹ requiring positron emission tomography (PET) with either a combination of ¹⁵O-labeled PET tracers or, more commonly, ¹¹C-acetate washout^{10–12} to assess MVO₂, combined with cardiac magnetic resonance imaging (CMR) or echocardiography to assess Cardiac Output (CO) and LV mass (LVM).

Since MEE integrates measurements of LV mass, function, and oxidative metabolism, a near-simultaneous acquisition of all measurements is preferred. This could be accomplished using hybrid PET/CMR or ECG-gated PET,¹³ but neither can be applied to all potential patient groups and both require significant post-processing of data, which would introduce observer bias. An optimal solution would be to extract CO and LVM directly from the dynamic PET data in an automated and scanner-independent fashion. Recently, automated methods of

obtaining forward cardiac output (FCO)¹⁴ and LVM¹⁵ have become available, using only a dynamic ¹¹C-acetate PET scan. Therefore, the aim of this study was to evaluate the accuracy of MEE derived from a single dynamic ¹¹C-acetate PET scan. In addition, obtained MEE values for patients with aortic valve stenosis (AVS) and mitral valve regurgitation (MVR) are compared with those of healthy controls.

MATERIALS AND METHODS

Patient Population

This study consists of a retrospective analysis of three groups of subjects undergoing efficiency measures in research studies from two different research sites. The first group consisted of 34 patients (69.0 ± 8.4y, 24 men) with AVS and varying degrees of heart failure (22 asymptomatic, 8 NYHA class II and 4 NYHA class III patients). All patients had sinus rhythm, no signs of myocardial ischemia and aortic valve area ≤ 1.2 cm² and/or transaortic maximal velocity of 3.0–5.0 m s⁻¹ based on echocardiography. The second group consisted of 20 patients (56.4 ± 15.6y, 19 men) with significant mitral regurgitation (regurgitant fraction > 30% on echocardiography) and with no or mild symptoms of heart failure (15 and five NYHA class I and II, respectively). The final group consisted of 10 healthy controls (62.5 ± 4.4y, 7 men) with no signs or history of cardiac disease. AVS patients and controls were scanned at the Aarhus University Hospital, Aarhus, Denmark whilst MVR patients were scanned at the Uppsala University Hospital, Uppsala, Sweden. The study was approved by the respective local ethical committees and all subjects gave written informed consent prior to inclusion in this study.

Image Acquisition

PET. ¹¹C-acetate synthesis was done according to Pike¹⁶ with minor in-house modifications. After a fasting period of > 4 h, AVS patients and controls underwent ¹¹C-acetate PET scan on a Siemens Biograph TruePoint TrueV 64 PET/CT scanner. Following a scout CT scan, a low-dose CT scan (120 kV, 30 mAs) was performed. After this, a 27-minute list mode emission scan was performed, starting simultaneously with automated injection of 407 ± 30 MBq ¹¹C-acetate as a 5–10 mL bolus (1 mL·s⁻¹) in a peripheral vein, followed by a 35-mL saline flush (2.0 mL·s⁻¹). List mode emission data were rebinned into a dynamic series consisting of 29 time frames using all data. Dynamic images were reconstructed using the TrueX algorithm, applying all appropriate corrections as supplied by the vendor.

MVR patients were scanned on a GE discovery ST with an acquisition protocol identical to that of AVS patients and controls. Data were reconstructed using the 3D IR algorithm with all appropriate corrections as supplied by the vendor.

CMR. AVS patients and controls were scanned on an Ingenia 1.5 T whole body scanner (Philips Healthcare, Best, The Netherlands) as described in¹⁴ and.¹⁵ MVR patients were

scanned on an Ingenia 3 T whole body scanner (Philips Healthcare, Best, The Netherlands) with an 80 mT·m⁻¹ gradient system, using similar imaging protocols. Details on exact settings can be found in the supplemental files.

Calculation of Myocardial External Efficiency

Myocardial external efficiency (MEE) was calculated using the methods as described in^{9,17} and the workflow used in this study is summarized in the supplemental file. MEE was defined as

$$MEE = \frac{EW}{TE} = \frac{MAP \cdot FCO \cdot 1.33 \cdot 10^{-4}}{MVO_2 \cdot LVM \cdot 20} \cdot 100\% \quad (1)$$

In which EW is the effective external work performed by the heart (J); TE is the total energy use (J); MAP is the mean arterial pressure (mmHg); FCO is the forward cardiac output (mL·min⁻¹); MVO₂ is the myocardial oxygen consumption (mL·g⁻¹·min⁻¹); LVM is the mass of the left ventricle (LV, g), and 1.33 · 10⁻⁴ and 20 are the conversion factors from 1 mmHg mL to J and from 1 mL of O₂ to J, respectively. The numerator, output energy (*E*_{out}) is similar to cardiac work, expressed in Joules, and represents the area enclosed within a pressure-volume loop. The denominator represents input energy (*E*_{in}), the total energy consumed by the LV.

HR and MAP were measured 1 minute before and 1 and 5 minutes after injection and averaged for calculation of MEE. MVO₂ was derived from ¹¹C-acetate PET data, whereas both FSV and LVM were derived from either CMR (FSV_{CMR} and LVM_{CMR}) or ¹¹C-acetate PET data (FSV_{PET} and LVM_{PET}). Supplemental Figure 1 summarizes the steps required for calculation of MEE, which are outlined below. An example of a dynamic time-series and all relevant intermediate steps of the analysis for each of the patient categories is shown in Supplemental Figures 2, 3, and 4.

MVO₂. PET scans were analyzed using aQuant¹⁸ (available at no cost for collaborative, non-commercial research purposes via <https://aquantsoft.com/go/aquantresearch>). Arterial (*C*_A(*t*)) and right-ventricular (*C*_{RV}(*t*)) blood concentrations were obtained automatically using cluster analysis.^{14,18} Arterial blood concentrations were converted into arterial plasma input functions (*C*_p(*t*)) by applying the average plasma metabolite correction as presented by Sun et al.¹⁹ Finally, *C*_p(*t*) was used for calculation of washout rate *k*₂ using a standard single compartment model²⁰ with all appropriate corrections for spillover from the blood and blood volume fractions:

$$C_{PET}(t) = (1 - V_A) \cdot K_1 \cdot C_p(t) \otimes e^{-k_2 \cdot t} + V_A \cdot C_A(t) + V_V \cdot C_V(t) \quad (2)$$

In which *C*_{PET}(*t*) represents the myocardial time-activity curve, and *C*_p(*t*), *C*_A(*t*), and *C*_{RV}(*t*) are the aforementioned blood time-activity curves. *V*_A represents arterial blood volume fraction (dimensionless), *K*₁ the uptake rate of ¹¹C-acetate in tissue (mL·g⁻¹·min⁻¹), *k*₂ the washout rate of ¹¹C-acetate (in min⁻¹), *V*_{RV} is the right-ventricular spillover fraction (dimensionless).

Parametric images were generated using basis function methods¹⁸ and used for automatic segmentation of the LV, as

described in detail elsewhere.¹⁵ In brief, for each short-axis slice the ventricular mid-point is defined using the center of gravity of *V*_A, from which radial profiles are generated every 10°. Then, for each profile, the first and last point above 2/3rd of the maximum of each profile were considered to represent the endo- and epicardial borders. This process was repeated for each profile and each short-axis slice until the entire LV was segmented.

After LV segmentation, activity concentrations in the LV were extracted and used as *C*_{PET}(*t*) in Eq. (2), yielding average *k*₂ of the entire LV. This global *k*₂ was converted into MVO₂ using the empirically derived conversion factors of Sun et al.¹⁹:

$$MVO_2 = 1.35 \cdot k_2 - 9.6 \cdot 10^{-3} \quad (3)$$

Identical values of MVO₂ were used for both MEE_{PET-CMR} and MEE_{PET}.

Forward cardiac output. For AVS patients and controls, CMR-based forward stroke volume (FSV_{CMR}) was calculated from phase contrast velocity measurement in the LV outflow tract. Flow analysis was performed using the freely available software Segment (version 1.9 R3746).²¹ As AVS regularly results in turbulent flow patterns, phase contrast velocity was imaged at the level of the LV outflow tract where flow velocity was laminar. For MVR patients, FSV_{CMR} was calculated from phase contrast velocity measurement in the ascending aorta and flow analyses were performed on a ViewForum workstation (Philips, Best, the Netherlands). FSV_{CMR} was multiplied with HR during PET to obtain FCO

FSV based on PET (FSV_{PET}) was calculated using indicator-dilution techniques using the methods described in¹⁴ correcting for scanner-dependent differences between FSV_{PET-CMR} and FSV_{PET} as presented in that study. In brief, the peak of the first-pass of the ¹¹C-acetate bolus through the arterial blood, obtained for calculation of MVO₂ as described above, was isolated automatically from *C*_A(*t*). Using this peak, forward cardiac output was estimated using

$$FCO_{PET} = \frac{I}{\int C_A(t)} \quad (4)$$

In which FCO_{PET} is forward cardiac output (mL·min⁻¹); *I* is the injected dose of ¹¹C-acetate (Bq) and $\int C_A(t)$ is the area under the curve of the isolated peak (Bq·mL⁻¹·min).

LVM. LVM_{CMR} was derived by manually tracing the endo- and epicardium in end-diastole on short-axis cine images tracing using the software Segment v1.9 R2854²¹ for AVS patients and ViewForum (Philips) for MVR patients. LVM_{PET} was defined using the volume of interest of the LV used to obtain *C*_{PET}(*t*). For both LVM_{PET-CMR} and LVM_{PET}, a density of myocardial tissue of 1.05 g cm³ was assumed.

Statistical Analysis

Data are presented as mean ± SD. Correlation and agreement were assessed using linear regression and Bland Altman plots. Paired *t* tests were used to evaluate systematic differences. Repeatability coefficient (RPC) was defined as 2 times the standard deviation of the difference. Differences between patient groups were assessed using One-way ANOVA

followed by student's *t* tests. The independent capacity of MEE_{PET} and MEE_{PET-CMR} for prediction of NYHA class was assessed by ordinal logistic fitting.

RESULTS

Data of one AVS patient showed significant motion during PET, and this patient was excluded from further analysis.

Patient Characteristics

Table 1 shows relevant hemodynamic parameters and all parameters used in calculation of MEE_{PET} for all three groups. Compared to controls, systolic blood pressure was significantly higher for AVS (*P* = 0.015) but not for MVR (*P* = 0.09). Neither MAP (*P* = 0.55 and 0.30) nor FCI (*P* = 0.27 and 0.17) were significantly different from controls, resulting in similar values for EW (*P* = 0.47 and 0.56 for AVS and MVR). MVO₂ in patients did not differ from that of controls (*P* = 0.26 and 0.92 for AVS and MVR) but LVM was larger (*P* = 0.003 and < 0.001), resulting in a significantly increased TE (*P* = 0.003 and 0.019).

Validation vs CMR

Correlation between PET and CMR was good for both FCO and LVM (*r* = 0.83 and *r* = 0.94, respectively, Figure 1). Correlation between PET- and CMR-derived measures was high for both EW and TE (*r* = 0.89, and 0.97, respectively, Figure 2). Bland

Altman analysis revealed no significant differences for EW (-1.2 ± 8.5 J, *P* = 0.445) or TE (3.4 ± 33.3 J, *P* = 0.564). Finally, correlation of MEE_{PET} and MEE_{PET-CMR} was high (*r* = 0.85, Figure 3) without significant bias (absolute difference of $-0.4 \pm 2.8\%$, *P* = 0.511).

EW_{PET} and EW_{PET-CMR} were not significantly different for any patient group. On the other hand, TE_{PET} was significantly higher than TE_{PET-CMR} for MVR (22.9 ± 26.0 J, *P* = 0.001) and significantly lower for controls (-28.1 ± 19.0 J, *P* = 0.001). Finally, MEE_{PET} was significantly different as compared to MEE_{PET-CMR} for controls ($2.8 \pm 3.0\%$, *P* = 0.02) and MVR ($-1.8 \pm 2.3\%$, *P* = 0.011) but not for AVS ($-0.2 \pm 2.6\%$, *P* = 0.62). Residual analysis identified the difference in FCO as the main source of difference in MEE in all groups (Controls: *r* = 0.58, *P* = 0.02; AVS: *r* = 0.79, *P* < 0.001; MVR: *r* = 0.58, *P* = 0.01).

Clinical Characteristics of MEE

When comparing patient groups, MEE_{PET} was significantly lower for both AVS (*P* < 0.001) and MVR (*P* = 0.006) as compared to controls (Figure 4), whilst MEE_{PET-CMR} was significantly lower for AVS (*P* = 0.009) but not MVR (*P* = 0.49). Mean aortic gradient in AVS was correlated to MEE_{PET-CMR} (*r* = -0.40, *P* = 0.023) and to MEE_{PET} (*r* = -0.62, *P* < 0.001, Figure 5), of which the correlation to MEE_{PET} was significantly higher (*P* = 0.01). In addition, regurgitant fraction was correlated to both MEE_{PET}

Table 1. Mean ± standard deviation of all hemodynamic or PET-derived parameters involved in calculation of myocardial external efficiency (MEE) for healthy controls, aortic valve stenosis (AVS), and mitral regurgitation (MVR) patients

	Controls (n = 10)	AVS (n = 33)	MVR (n = 20)
SBP (mmHg)	124 ± 11	139 ± 18*	134 ± 15
DBP (mmHg)	79 ± 6	79 ± 11	71 ± 13 [†]
HR (min ⁻¹)	62 ± 8	65 ± 11	60 ± 12
MAP (mmHg)	97 ± 9	99 ± 12	92 ± 12 [†]
MVO ₂ (mL _{O2} ·g ⁻¹ ·min ⁻¹)	0.10 ± 0.02	0.12 ± 0.04	0.11 ± 0.03
FCI (L·min ⁻¹ ·m ⁻²)	2.4 ± 0.4	2.6 ± 0.6	2.6 ± 0.4
LVMi (g·m ⁻²)	63.8 ± 8.4	89.3 ± 25.0**	90.5 ± 17.2***
EW (J)	60.9 ± 15.0	66.2 ± 21.0	64.3 ± 14.6
TE (J)	260 ± 57	399 ± 137**	385 ± 152*
MEE (%)	23.6 ± 4.2	17.2 ± 4.3***	18.0 ± 5.2**

SBP, systolic blood pressure; DBP, diastolic blood pressure; HR, heart rate; MAP, mean arterial pressure; MVO₂, rate of oxygen consumption; FCI, forward cardiac index; LVMi, left ventricular mass corrected for body-surface area; EW, external work; TE, total energy usage

*, ** and ****P* < 0.05, < 0.01 and < 0.001 vs healthy controls

[†]*P* < 0.05 vs AVS

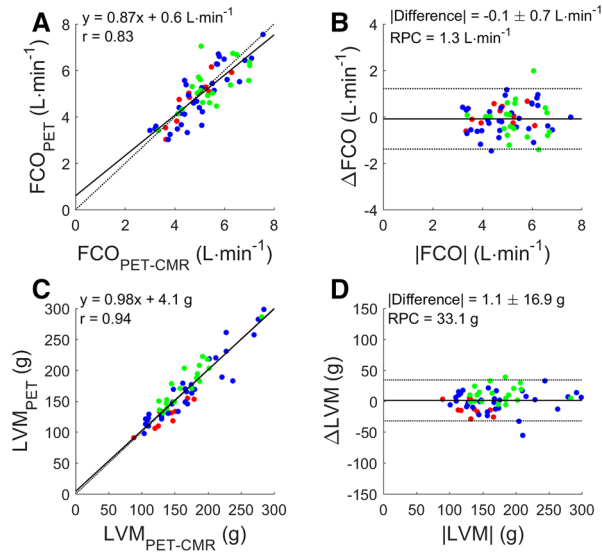


Figure 1. Correlation (A, C) and Bland Altman plot (B, D) of forward cardiac output (A, B) and left ventricular mass (C, D) based on CMR (FCO_{PET-CMR} and LVM_{PET-CMR}) and PET (FCO_{PET} and LVM_{PET}). Black and gray lines indicate the line of identity and the linear fit in (A, C) and the mean difference and the 95% confidence interval in (B, D). RPC: repeatability coefficient. Red: healthy controls ($n = 10$), blue: AVS patients ($n = 33$), green: MVR patients ($n = 20$).

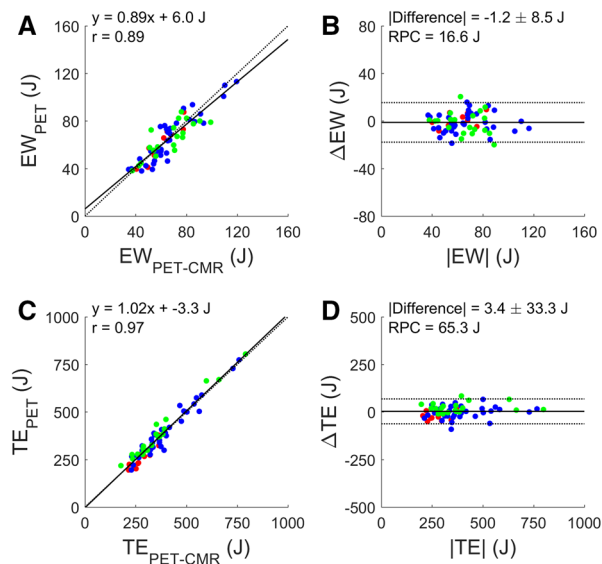


Figure 2. Correlation (A, C) and Bland Altman plot (B, D) of external work (A, B) and total energy use (C, D) based on CMR (EW_{PET-CMR} and TE_{PET-CMR}) and PET (EW_{PET} and TE_{PET}). Black and gray lines indicate the line of identity and the linear fit in (A, C) and the mean difference and the 95% confidence interval in (B, D). RPC, repeatability coefficient. Red: healthy controls ($n = 10$), blue: AVS patients ($n = 33$), green: MVR patients ($n = 20$).

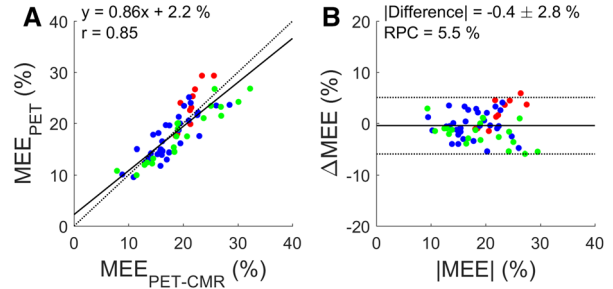


Figure 3. Correlation (A) and Bland Altman plot (B) of myocardial external efficiency based on a combined PET-CMR protocol (MEE_{PET-CMR}) and PET-only (MEE_{PET}). Black and gray lines indicate the line of identity and the linear fit in (A) and the mean difference and the 95% confidence interval in (B). RPC: repeatability coefficient. Red: healthy controls ($n = 10$), blue: AVS patients ($n = 33$), green: MVR patients ($n = 20$).

($r = -0.61$, $P = 0.009$) and to MEE_{PET-CMR} ($r = -0.49$, $P = 0.045$, Figure 6) with no significant difference between correlations ($P = 0.10$). Finally, MEE_{PET} was strongly associated with NYHA class (ANOVA $P < 0.001$) and significantly separated most groups (Figure 7), while the association was less clear for MEE_{PET-CMR} (ANOVA $P = 0.03$). Using Ordinal Logistic fitting only MEE_{PET} was independently associated with NYHA class (χ^2 14.2, $P < 0.0002$), compared to MEE_{PET-CMR} (χ^2 3.8, $P = 0.052$).

DISCUSSION

This study presents a fully automated method of calculating myocardial external efficiency (MEE) solely from a dynamic ¹¹C-acetate PET/CT scan without the use of ECG-gating. This method eliminates the need for separate measurements of cardiac output and LV mass, reducing protocol duration, cost and analysis time. MEE is a sensitive marker of cardiac performance and has been used as surrogate end-point in several interventional studies,^{7,8} potentially lowering the sample size as compared to traditional markers such as ejection fraction or outcomes.

Both FCO and LVM have been validated vs CMR before^{14,15} in a subset of the subjects included in this study. LVM measured by PET without ECG-gating in particular appears to perform well across different scanners, compared to CMR. FCO requires a scanner-dependent correction factor, as previously observed.¹⁴ The difference in FCO was identified as the only significant source of MEE deviation between modalities. Since associations towards clinical parameters were stronger for MEE_{PET}, the difference in FCO points to a

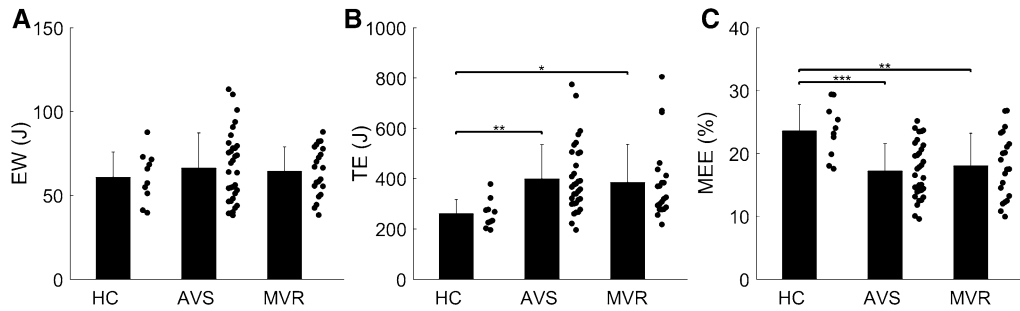


Figure 4. Mean ± SD and individual values for EW_{PET} (A), TE_{PET} (B) and MEE_{PET} (C) for all three groups. *, **, *** indicate significance level of < 0.05, < 0.01, and < 0.001, respectively.

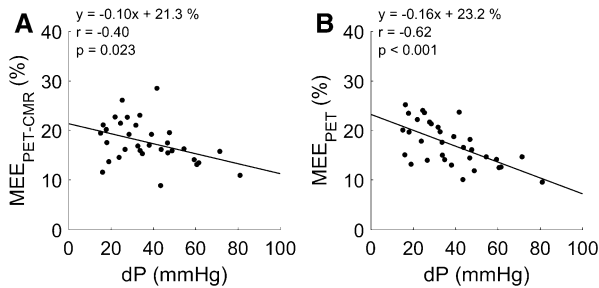


Figure 5. Correlation of mean pressure gradient over de aortic valve and MEE derived using PET-CMR (A) and PET-only (B) for AVS patients.

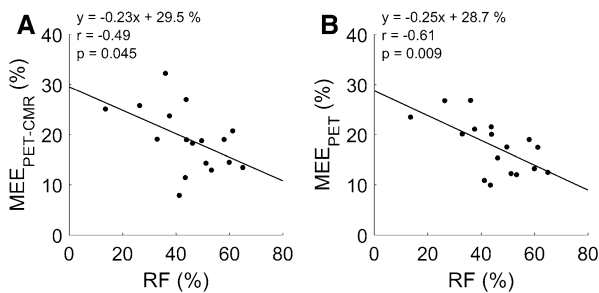


Figure 6. Correlation of CMR-derived regurgitant fractions and MEE derived using PET-CMR (A) and PET-only (B) for MVR patients. *RF*, regurgitant fraction.

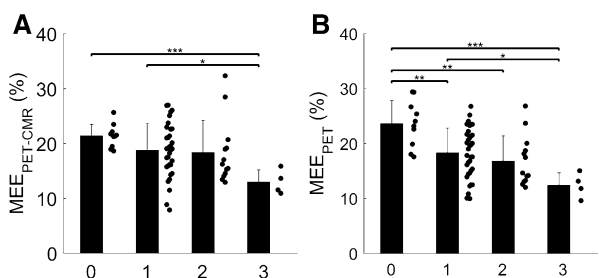


Figure 7. Mean ± standard deviation of MEE_{PET-CMR} (A) and MEE_{PET} (B) per NYHA heart failure class. *, **, and *** denote a *P* value below 0.05, 0.01, and 0.001, respectively.

significant change in LV loading conditions between the CMR and PET scans. This is encouraging in terms of using MEE from PET alone as an end-point in multi-center trials, but including other scanner models requires further validation against CMR to establish correction factors.

In a test-retest study, we show that repeatability of MEE_{PET-CMR} and MEE_{PET} were high and not significantly different (coefficient of variation of 6.3% and 9.5%, respectively, *P* = 0.25).²² The range of control values was narrower for MEE_{PET-CMR} as compared to MEE_{PET}, as can also be appreciated in Figure 7, suggesting a higher sensitivity and the need for smaller groups when using MEE_{PET-CMR} as marker for efficiency. However, Figure 7 also shows that the difference between controls and patients with valvular diseases was higher for MEE_{PET}, suggesting that the (non-significantly) increased test-retest variability for MEE_{PET} is largely off-set by an increased effect size. The exact benefit of using either MEE_{PET} and MEE_{PET-CMR} must be studied in larger clinical studies. Finally, the use of a combined PET-echocardiography protocol was not recommended from a reproducibility point of view.²²

MEE calculated with both approaches resulted in control values ranging from 17 to 30%, which is in line with previously published invasive measurements.⁹ Patients were consecutively recruited from on-going larger studies and two-thirds were asymptomatic. Half of the patients had MEE lower than any control subject, suggesting that attenuated efficiency at rest is common in valvular diseases. MEE_{PET} was significantly correlated to the echocardiographically derived mean pressure gradient of the aortic valve in AVS patients (*r* = - 0.62, *P* < 0.001) and to the regurgitant fraction obtained from CMR in MVR patients (*r* = - 0.61, *P* = 0.009). In addition, MEE corresponded to the subjective level of disease burden defined by the NYHA class. This indicates that MEE reflects the phenotypic response to the causative disease process in valvular

disease. To what extent MEE can be used to define the optimal time point for valvuloplasty requires larger outcome studies, for which the current study suggests that a PET-alone approach might perform better than serial multimodality imaging.

Care has to be taken when comparing different values for MEE in literature. In some studies, pressure gradient over the aortic valve is used in Eq. (1) (replacing MAP by MAP+ Δ P), which is likely to minimize differences in MEE. Similarly, when the total stroke volume including the blood that regurgitates over either valve is used instead of FSV, differences between controls and MVR are expected to be smaller and it becomes clear that there are conceptual differences between MEE obtained in either case. MEE as calculated using Eq. (1) represents the energetic cost of the entire LV required to pump a certain amount of blood into the systemic circulation, ignoring any pathological pressures in the LV cavity and excluding any regurgitating volume. This could be considered the net efficiency of the whole heart as a pump or *global LV efficiency* and reflects both the metabolic and mechanical state of the heart. The result of this study suggests that global LV efficiency is a sensitive marker of generic cardiac performance. If, on the other hand, regurgitation or elevated LV pressures are taken into account, MEE represents the energetic cost of displacing blood in any direction which can be considered the efficiency of the cardiomyocytes, reflecting the metabolic state of the heart specifically i.e., the *metabolic efficiency*. Noteworthy, global LV and metabolic efficiency deviate only in the case of valvular dysfunction. When pressure gradients are essential, echocardiography can be performed during a PET examination,²³ although echocardiography is limited by the acoustic window and the presence of significant operator differences. Similarly, total stroke volume can be obtained using gated PET but accuracy of that method is so far suboptimal.¹³ However, the present study shows that it is feasible to obtain MEE according to either definition during a single scan session.

This study has several limitations that need to be acknowledged. The PET acquisition protocols were aligned between both participating sites, but since differences between PET scanners were observed widespread implementation of this all-in-one approach in multicenter studies requires further validation. CMR equipment and protocols differed between sites, which is likely to induce bias.

Secondly, this study mainly included subjects with valvular abnormalities which typically show discrepancies in pressure-volume loops. The assumption that EW, formally defined as the area encompassed in a patient's pressure-volume loop, can be approximated by the

product of MAP and SV is often incorrect in these patients.⁹ Errors in EW estimates can be reduced by utilizing forward instead of total stroke volume and/or adding the mean pressure gradient over the aortic valve, although the latter increases complexity of the method. As discussed above, care has to be taken when considering the use of mean pressure gradients or whether to use the forward or total stroke volume. In this study, we chose to use forward stroke volume and exclude mean pressure gradient to obtain a 'net' or global LV efficiency, equally affected by mechanical abnormalities of the heart and valves and by any potential metabolic alterations.

To conclude, myocardial efficiency can be measured accurately using a single ¹¹C-acetate PET/CT scan, without the need for additional imaging modalities. Because of the more generic, highly automated, and less logistically demanding approach, this novel technique might widen the applicability of MEE to more patient groups.

NEW KNOWLEDGE GAINED

The work presented in this study enables a simplified, faster, and more automated assessment of myocardial external efficiency using a single ¹¹C-acetate scan. Using a single scan protocol instead of a combined PET-CMR protocol leads to lower potential errors due to differences in loading conditions. When applying this method to a cohort of controls and patients with valvular diseases, MEE based on PET-only correlated more closely to the underlying disease state and to NYHA class.

Acknowledgments

This study was supported financially by the Lundbeck Foundation, Arvids Nilssons Foundation, Karen Elise Jensens Foundation, the Snedkermester Sophus Jacobsen & Hustru Astrid Jacobsens Foundation, the Health Research Fund of Central Denmark Region and the Swedish Heart-Lung Foundation.

Disclosure

None of the authors have any conflicts of interest to declare.

Open Access

This article is distributed under the terms of the Creative Commons Attribution 4.0 International License (<http://creativecommons.org/licenses/by/4.0/>), which permits unrestricted use, distribution, and reproduction in any medium, provided you give appropriate credit to the original author(s) and the source, provide a link to the Creative Commons license, and indicate if changes were made.

References

1. Ingwall JS, Weiss RG. Is the failing heart energy starved? On using chemical energy to support cardiac function. *Circ Res* 2004;95:135–45.
2. Beanlands RS, Nahmias C, Gordon E, et al. The effects of beta(1)-blockade on oxidative metabolism and the metabolic cost of ventricular work in patients with left ventricular dysfunction: a double-blind, placebo-controlled, positron-emission tomography study. *Circulation* 2000;102:2070–5.
3. Beanlands RS, Bach DS, Raylman R, et al. Acute effects of dobutamine on myocardial oxygen consumption and cardiac efficiency measured using carbon-11 acetate kinetics in patients with dilated cardiomyopathy. *J Am Coll Cardiol* 1993;22:1389–98.
4. Sugiki T, Naya M, Manabe O, et al. Effects of surgical ventricular reconstruction and mitral complex reconstruction on cardiac oxidative metabolism and efficiency in nonischemic and ischemic dilated cardiomyopathy. *JACC Cardiovasc Imaging* 2011;4:762–70.
5. Güçlü A, Knaapen P, Harms HJ, et al. Myocardial efficiency is an important determinant of functional improvement after aortic valve replacement in aortic valve stenosis patients: a combined PET and CMR study. *Eur Heart J Cardiovasc Imaging* 2015;16:882–9.
6. Timmer SAJ, Knaapen P. Coronary microvascular function, myocardial metabolism, and energetics in hypertrophic cardiomyopathy: insights from positron emission tomography. *Eur Heart J Cardiovasc Imaging* 2013;14:95–101.
7. Chen WJY, Diamant M, de Boer K, et al. Effects of exenatide on cardiac function, perfusion, and energetics in type 2 diabetic patients with cardiomyopathy: a randomized controlled trial against insulin glargine. *Cardiovasc Diabetol* 2017;16:67.
8. Hansson NH, Sörensen J, Harms HJ, et al. Metoprolol reduces hemodynamic and metabolic overload in asymptomatic aortic valve stenosis patients: a randomized trial. *Circ Cardiovasc Imaging* 2017;10:e006557.
9. Knaapen P, Germans T, Knuuti J, et al. Myocardial energetics and efficiency: current status of the noninvasive approach. *Circulation* 2007;115:918–27.
10. Brown M, Marshall DR, Sobel BE, Bergmann SR. Delineation of myocardial oxygen utilization with carbon-11-labeled acetate. *Circulation* 1987;76:687–96.
11. Buxton DB, Schwaiger M, Nguyen A, et al. Radiolabeled acetate as a tracer of myocardial tricarboxylic acid cycle flux. *Circ Res* 1988;63:628–34.
12. Armbrecht JJ, Buxton DB, Schelbert HR. Validation of [1-¹¹C]acetate as a tracer for noninvasive assessment of oxidative metabolism with positron emission tomography in normal, ischemic, postischemic, and hyperemic canine myocardium. *Circulation* 1990;81:1594–605.
13. Hansson NH, Tolbod L, Harms HJ, et al. Evaluation of ECG-gated [11C]acetate PET for measuring left ventricular volumes, mass, and myocardial external efficiency. *J Nucl Cardiol* 2016;23:670–9.
14. Harms HJ, Tolbod LP, Hansson NHS, et al. Automatic extraction of forward stroke volume using dynamic PET/CT: a dual-tracer and dual-scanner validation in patients with heart valve disease. *EJNMMI Phys* 2015;2:25.
15. Harms HJ, Stubkjær Hansson NH, Tolbod LP, et al. Automatic extraction of myocardial mass and volume using parametric images from dynamic nongated PET. *J Nucl Med* 2016;57:1382–7.
16. Pike VW, Eakins MN, Allan RM, Selwyn AP. Preparation of [1-¹¹C]acetate—an agent for the study of myocardial metabolism by positron emission tomography. *Int J Appl Radiat Isot* 1982;33:505–12.
17. Porenta G, Cherry S, Czernin J, et al. Noninvasive determination of myocardial blood flow, oxygen consumption and efficiency in normal humans by carbon-11 acetate positron emission tomography imaging. *Eur J Nucl Med* 1999;26:1465–74.
18. Harms HJ, Knaapen P, De Haan S, et al. Automatic generation of absolute myocardial blood flow images using [(15)O]H₂O and a clinical PET/CT scanner. *Eur J Nucl Med Mol Imaging* 2011;38:930–9.
19. Sun KT, Yeatman LA, Buxton DB, et al. Simultaneous measurement of myocardial oxygen consumption and blood flow using [1-carbon-11]acetate. *J Nucl Med* 1998;39:272–80.
20. Timmer SA, Lubberink M, van Rossum AC, et al. Reappraisal of a single-tissue compartment model for estimation of myocardial oxygen consumption by [11C]acetate PET: an alternative to conventional monoexponential curve fitting. *Nucl Med Commun* 2011;32:59–62.
21. Heiberg E, Sjögren J, Ugander M, et al. Design and validation of Segment—freely available software for cardiovascular image analysis. *BMC Med Imaging* 2010;10:1.
22. Hansson NH, Harms HJ, Kim WY et al. Test-retest repeatability of myocardial oxidative metabolism and efficiency using standalone dynamic ¹¹C-acetate PET and multimodality approaches in healthy controls. *J Nucl Cardiol*. 2018. <https://doi.org/10.1007/s12350-018-1302-z>.
23. Ukkonen H, Saraste M, Akkila J, et al. Myocardial efficiency during calcium sensitization with levosimendan: a noninvasive study with positron emission tomography and echocardiography in healthy volunteers. *Clin Pharmacol Ther* 1997;61:596–607.